

# Time dependent behavior of CO<sub>2</sub> hydrate-bearing sediments and its modelling by an elasto-viscoplastic model

Sayuri Kimoto<sup>1\*</sup>, Yota Konishi<sup>2</sup>, Hiromasa Iwai<sup>3</sup>, Yuguang Wu<sup>2</sup>, Masaki Yoshimoto<sup>1</sup>, Gyo Takubo<sup>1</sup>

<sup>1</sup> Kyoto University, Kyoto, Japan

<sup>2</sup> Former student of Kyoto University, Kyoto, Japan

<sup>3</sup> Nagoya Institute of Technology, Nagoya, Japan

\* kimoto.sayuri.6u@kyoto-u.ac.jp

## Introduction

The first and second offshore gas production tests from hydrate sediments were conducted at Daini-Atsumi knoll, Eastern Nankai Trough, Japan in 2014 and 2017, respectively. It is reported that methane hydrates were dissociated by depressurization and gas was produced. The more technical challenges are, however, needed for the long-term and economical production. A possible technique to enhance gas productivity is CO<sub>2</sub> injection into hydrate bearing sediments. The reaction heat of CO<sub>2</sub> hydrate formation can promote methane gas dissociation, in addition, CO<sub>2</sub> can be stored as hydrates in seabed ground by CH<sub>4</sub>-CO<sub>2</sub> exchange. In the present study, the mechanical behavior of CO<sub>2</sub> hydrate bearing sediments was investigated to provide the fundamental mechanical properties of CO<sub>2</sub> hydrate sediments. Especially, time dependent behavior was focused on and a series of undrained triaxial tests were conducted using high pressure and low temperature triaxial apparatus. In addition, an elasto-viscoplastic model considering the effect of hydrate saturation is adopted to reproduce the test results.

## Undrained creep tests for CO<sub>2</sub> hydrate-bearing sediments

A high-pressure and low-temperature triaxial apparatus (Iwai 2015) which has been designed to investigate the geo-mechanical behavior of gas hydrate-bearing soils was used for the undrained creep triaxial tests. Toyoura silica sand was chosen for the host soil material, and the moist sand with a water content of 16% was compacted by a tamper to make the specimen with 35 mm diameter and 70 mm in height. Then, the specimen was subjected to the formation process of CO<sub>2</sub>-hydrates in the triaxial cell by controlling the temperature and the pressure. After generating CO<sub>2</sub>-hydrates, the specimen was saturated with water. The cell pressure and the back pressure were set to 12 MPa and 10 MPa, respectively, so that the effective confining pressure was set to be 2 MPa. After the consolidation process, the constant axial strain rate of 0.5 %/min was applied to the specimen under undrained condition until the deviator stress reached to the creep stress. Then, the creep tests were started. Three specimens with the different hydrate saturation were tested as shown in Table 1. The hydrate saturation is defined as:

$$S_r^H = V^H / V^v \times 100 \text{ [%]} \quad (1)$$

where  $V^H$  and  $V^v$  are the volume fraction of the hydrates and the void respectively. The creep stress ratio  $q_r$  is defined by the following equation:

$$q_r = q / q_{max} \quad (2) \quad q_{max} = 0.0496 (S_r^H)^{1.46} + 4.19 \quad (3)$$

where the strength  $q_{max}$  depends on the hydrate saturation and it is estimated by Eq. (3) by the existing data of undrained compression tests. Case S is the case of water-saturated sand sample without hydrate.

**Table 1: Test conditions**

	Hydrate saturation $S_r^H$ [%]	Creep stress $q$ [MPa]	Creep stress ratio $q_r$
Case S	0.0	3.5	0.84
Case H1	21.8	4.0	0.86
Case H2	40.0	4.0	0.71

## Simulations by an elasto-viscoplastic constitutive model

An elasto-viscoplastic model based on the overstress type of viscoplastic theory with the nonlinear kinematic hardening rules considering the effect of hydrate (Akaki et al. 2016) were adopted. The effect of hydrate saturation was introduced in the elastic shear modulus and the viscoplastic parameters base on the test results. The elastic shear modulus was given as

$$G_0 = G_{0s} + n_g S_r^H \quad (4) \quad G = \left[ \frac{G_0}{1 + \alpha^b (\gamma^{vp})^c} \right] \sqrt{\frac{\sigma'_m}{\sigma'_{m0}}}, \quad b = 1 + S_r^H \quad (5)$$

where  $n_g$ ,  $r$  are the material parameters for the hydrate saturation dependency,  $G_{0s}$  is an elastic shear modulus for sand without hydrate,  $\gamma^{vp}$  is an accumulated viscoplastic deviatoric strain. As for the viscoplastic strain, the strain hardening-softening parameter  $\sigma'_{mb}$  in the overconsolidated boundary surface and the static yield surface are given as

$$\sigma'_{mb} = N_m \sigma'_{ma} \exp\left\{(1 + e_0/\lambda - \kappa)\varepsilon_{kk}^{vp}\right\} \quad (6) \quad N_m = 1 + n_m \cdot (S_r^H)^{nd} \quad (7)$$

$$\sigma'_{ma} = \sigma'_{maf} + (\sigma'_{mai} - \sigma'_{maf})\exp(-\beta z), \quad z = \int_0^t \dot{z} dt, \quad \dot{z} = \sqrt{\dot{\varepsilon}_{ij}^{vp} \dot{\varepsilon}_{ij}^{vp}} \quad (8)$$

where  $\varepsilon_{kk}^{vp}$  is the accumulated viscoplastic volumetric strain,  $\dot{\varepsilon}_{ij}^{vp}$  is the viscoplastic strain rate tensor,  $\sigma'_{maf}$  and  $\beta$  are the material parameters regarding to the structural degradation. The viscoplastic parameters,  $m'$ ,  $C_1$ ,  $C_2$ , are given as functions of hydrate saturation as

$$m' = 1 / \left( 1/m'_s + m_b \cdot (S_r^H)^{m_c} \right) \quad (9) \quad C_1 = C_{1s} \left\{ 1 + c_{1b} \cdot (S_r^H)^{c_{1c}} \right\} \quad (10) \quad C_2 = C_1 / (C_{2s}/C_{1s} + c_{2b} \cdot S_r^H) \quad (11)$$

in which  $m'_s$ ,  $C_{1s}$ ,  $C_{2s}$  are the values of  $m'$ ,  $C_1$ ,  $C_2$  for sand. The material parameter  $\beta$  is set to be 0, 2.65, and 7.25 for the Case S, Case H1, and Case H2, respectively.

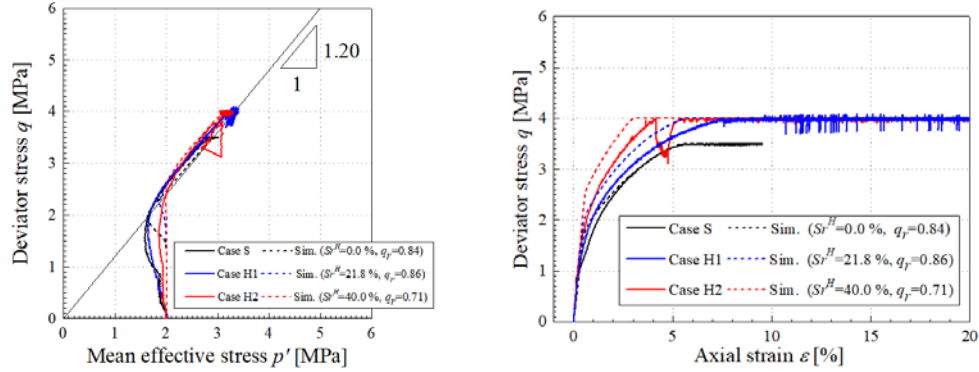


**Fig. 1: Effective stress paths and stress-strain relations**

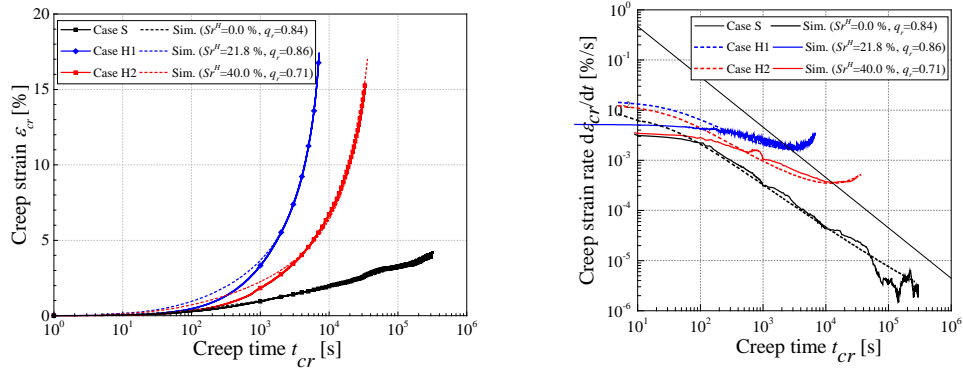


**Fig. 2: Time-strain and time-strain relations during creep**

The test results and the simulations are compared in Figs. 1 and 2. The steady creep and the acceleration creep are observed for the hydrate-bearing specimen, whereas the strain rate decreases constantly for the case of sand specimen. The simulations well reproduce the behavior during undrained creep including the steady creep and the acceleration creep except the stress-strain relations before creep.

## Conclusion

A series of undrained creep tests were conducted for hydrate-bearing sandy specimens and the results were compared with simulations by the elasto-viscoplastic model. It is found that the model considering the effect of hydrate saturation can well reproduce the creep behavior of hydrate-bearing soil.

## References

- Iwai H (2015) Behavior of gas hydrate-bearing soils during dissociation and its simulation. Ph. D. thesis, Kyoto University  
 Akaki T, Kimoto S, Oka F (2016) Chemo-thermo-mechanically coupled seismic analysis of methane hydrate-bearing sediments during a predicted Nankai Trough Earthquake. Int. J. Numer. Anal. Meth. Geomech. 40:2207–2237